

Supporting Information

3D Printing Polymerizable Eutectics via RAFT Polymerization

Nathaniel Corrigan,^{a,*} Alexandra L. Mutch,^b Cyrille Boyer,^{a,*} and Stuart C. Thickett^{b,*}

^aCluster for Advanced Macromolecular Design (CAMD) and Australian Centre for NanoMedicine (ACN),
School of Chemical Engineering, University of New South Wales, Sydney, NSW 2052, Australia.

^bSchool of Natural Sciences (Chemistry), University of Tasmania, Hobart, Tasmania 7005, Australia

Email: n.corrigan@unsw.edu.au, cboyer@unsw.edu.au, stuart.thickett@utas.edu.au

Materials

Unless otherwise stated, all materials were used as received. Monomers: *N*-isopropylacrylamide (NIPAm, 97%), Acrylamide (Am, $\geq 99\%$), methylenebisacrylamide (MBAm, 99%), and poly(ethylene glycol) diacrylate (PEGDA 250, average $M_n = 250 \text{ g mol}^{-1}$) were purchased from Merck. RAFT agents: 4-(((2-carboxyethyl)thio)carbonothioyl)thio)-4-cyanopentanoic acid (CTCPA, 95%), 2,2'-(carbonothioylbis(thio))bis(2-methylpropanoic acid (BisPAT, 97%), dibenzyl trithiocarbonate (DBTTC, 99%) were purchased from Boron Molecular. Solvents: absolute ethanol was purchased from Thermo Fisher Scientific, deionized water was dispensed from a Satorius arium pro ultrapure water system operating at $18.2 \text{ M}\Omega \cdot \text{cm}$. Photoinitiator: Diphenyl(2,4,6-trimethylbenzoyl)phosphine oxide (TPO, 97%) was purchased from Merck. Thermal initiator: Azobisisobutyronitrile (AIBN, 12 wt% solution in acetone) was purchased from Merck and evaporated to dryness under vacuum. The dried crystalline powder was directly used.

Methods

PE Resin preparation

Preparation of PE resins was performed using the general procedure outlined here for the 0.5 wt% BisPAT resin. To a 100 mL amber flask equipped with a magnetic stir bar was added 34.79 g NIPAm (0.307 mol), 7.28 g Am (0.102 mol), and 4.68 g H_2O (0.259 mol). The amber vial was sealed with a rubber septum, parafilm, and iron wire, then placed in a pre-heated oil bath set to $50 \text{ }^\circ\text{C}$ with stirring at 600 rpm. The mixture was stirred for 1 h then the oil bath was turned off while the amber vial remained in the oil. After 30 min the amber vial containing the now liquid PE was removed. To this PE solution was added 2 g MBAm (13.0 mmol), 1 g TPO (2.87 mmol) and 0.25 g BisPAT (0.89 mmol). This mixture was stirred at room temperature for 30 min until the added solid components had dissolved and the solution appeared visually transparent. This resin, in this case the 0.5 wt% BisPAT resin, was used directly for 3D printing.

Viscosity measurements

The viscosity of the base PE mixture was measured using a Brookfield DV3T (LVCI) Rheometer using a CP-42 (42z) spindle and temperature controlled using a TC-150SD heating apparatus. The analysis was performed at speed of 20 rpm, which provided a torque of 49.3%. The temperature was maintained at $25.5 \text{ }^\circ\text{C}$ for the duration of testing.

Differential scanning calorimetry (DSC)

DSC was performed to analyze the freezing point of the base mixture, which was a liquid at room temperature. DSC experiments were performed using a TA instruments Q20 DSC instrument equipped with an RCS40 refrigerated cooling system. The DSC run was performed by heating the sample to $60 \text{ }^\circ\text{C}$ at a rate of $5 \text{ }^\circ\text{C}$

min⁻¹, followed by an isothermal hold for 10 min, then a cooling cycle to -30 °C at a rate of 2 °C min⁻¹. Another isothermal hold was performed at -30 °C for 10 min, followed by a heating ramp to 60 °C at a rate of 2 °C min⁻¹. The resulting DSC curve (shown as one full cooling -heating cycle from 60 °C to -30 °C to 60 °C) is shown in **SI Figure S1**. The freezing point was determined as the onset of the exothermic transition during the cooling cycle, taken as the intersection of the tangent of the cooling curve prior to the onset, and the tangent of the exothermic peak. The frozen base mixture showed a melting point of 24°C, determined via the same method, albeit on the heating cycle.

Attenuated total reflectance-Fourier transform infrared spectroscopy

ATR-FTIR was performed to estimate the speed of polymerization for systems containing no-RAFT, 0.5 wt% BisPAT, and 1.0 wt% BisPAT. A Bruker Alpha ATR-FTIR spectrophotometer equipped with room temperature DTGS detectors was used for measurement. Each spectrum was obtained using 4 scans with a resolution of 4 cm⁻¹ and was collected in the spectral region between 4000-400 cm⁻¹. Analysis was performed using OPUS software. These experiments were performed in triplicate and the data were presented as an average conversion at each time point. A 15 uL droplet was dropped directly onto the ATR-FTIR crystal plate, then exposed top-down with a ThorLabs 405 nm LED light with a collimation adaptor. The light intensity was measured to be 0.81 mW cm⁻² at the polymerization surface. The droplet was irradiated at irregular intervals depending on the resin being analysed. The peak from 1403-1433 cm⁻¹, corresponding to the =CH₂ scissoring mode of the monomers was monitored. This wavenumber range was selected as these are isosbestic points during the transition from monomer to polymer. The fractional conversion was calculated by taking the ratio of the integral of this peak at time t, to the integral of this peak at time 0, and then subtracting this ratio from 1. A representative kinetic set from FTIR for the BisPAT 1.0 sample is presented in **SI Figure S2**. These conditions demonstrated the suitability for the selection of 15, 30 and 45 s cure times for the no-RAFT, BisPAT 0.5, and BisPAT 1.0 resin systems, respectively, as the double bond conversions were high after these points. It should be noted that this setup is not a direct match for 3D printing, as the FTIR setup uses droplets that are fully open to air. Thus, the cure time via FTIR is likely to be longer than in the 3D printer.

Fourier transform near-infrared spectroscopy (FTNIR)

FTNIR was performed to provide a quantitative measure of the double bond conversion for 3D printed PE samples. A Bruker Vertex 70 FTNIR was used for all measurements, using a scan range of 4000-12000 cm⁻¹, and with 16 scans per sample. Measurements were performed both before and after the 15 min post cure process. Prior to analysis, the liquid resins were measured using a 2 mm path length cuvette. The integral of the vinylic C-H stretching overtone in the range of 6100-6240 cm⁻¹ was measured, and used for calibration. The 3D printed samples were measured using digital callipers (thickness), and then the integral in the same wavelength range was measured. The final integral was normalized to provide a quantitative measurement of

the vinyl bond conversion, relative to a 2 mm thick sample. Samples had thickness in the range of 0.87-1.04 mm. All conversions were high (>94%) directly after the 3D printing process. The individual FTNIR curves for these samples are shown in **Figure S4**.

3D printing pre-polymer layer

A mixture of 2 wt% TPO in pure PEGDA 250 was prepared, sonicated and vortexed to ensure homogeneity. Prior to 3D printing of the PE mixtures, a commercial light-based 3D printer (Anycubic Photon S, 405 nm LED light array, $I_0 = 0.81 \text{ mW cm}^{-2}$ at print surface) was used to cure a 50×50 mm (x, y) layer of PPEGDA 250 onto the centre of the build stage. The cure time for this single layer was 60 s and the layer thickness was 50 μm . The build stage was removed and briefly washed with ethanol, then the entire build stage was post-cured under a 405 nm flood curing lamp for 30 min. The build stage was then placed back into the 3D printer and the stage was levelled again, with the PPEGDA layer still attached to the build plate. The 3D printing of the PE materials was then performed as usual. Following 3D printing of the PE materials, the objects were briefly washed with ethanol and then post-cured under a 405 nm flood curing lamp, while still on the build plate, for 30 min. The PE materials and the PPEGDA sacrificial layer were removed as one, then the PPEGDA layer was carefully peeled away from the PE materials manually using a 0.1 mm thick phone screen separator.

3D printing

The targeted material geometries and .stl files were generated using Autodesk Fusion, and printing parameters (slicing thickness and layer cure times) were generated using Photon Workshop software. The LCD digitally masked DLP 3D printer (Anycubic Photon S) used an LED light array emitting 0.81 mW cm^{-2} violet light ($\lambda_{\text{max}} = 405 \text{ nm}$) at the polymerization surface, as measured using a Newport 843-R power meter. Prior to printing of the PE materials, unless otherwise noted, a 50 μm layer of PEGDA 250 was polymerized onto the build stage using the procedure outlined in the “3D printing pre-polymer layer” section. The lattice shown in the main text, Figure 7, was 3D printed using an Anycubic MonoX printer, adjusted to the same light intensity as the Photon S printer (0.81 mW cm^{-2} violet light, $\lambda_{\text{max}} = 405 \text{ nm}$). All other printing conditions, i.e., cure time, layer thickness, Z-lift and retract speeds, and Z-lift distance, were the same for all prints, as detailed below.

All PE materials were printed using four bottom layers with cure times of 30, 45, and 60 s, respectively, for the no-RAFT, 0.5 wt% and 1.0 wt% BisPAT resins. The regular cure time per layer was 15, 30, and 45 s for the no-RAFT, 0.5 wt% and 1.0 wt% BisPAT resins, respectively. The Z lift distance was 6 mm, the Z lift speed was 2 mm s^{-1} , and the Z retract speed was 4 mm s^{-1} . After the object was printed, the build stage was removed, and the build stage and 3D printed material were briefly washed with ethanol. The material was then post-cured for 15 min under violet light ($\lambda_{\text{max}} = 405 \text{ nm}$, $I_0 = 9.6 \text{ mW cm}^{-2}$).

Procedure for thermally curing PE mixtures between aluminium laps

6061-type aluminium laps with dimensions of $100 \times 25.4 \times 1$ mm (l, w, t) were machined in house at UNSW Sydney. The laps were cleaned by brief immersion in 1 M HCl for 5 min, then further cleaned with isopropanol prior to use. A 25.4 mm square was marked on the end of each lap, then 50 μ L of the PE solution was cast onto one of the squares. The 25.4 mm square of another aluminium lap was placed over the PE droplet and held in place with two butterfly clips (20 mm) on each side of the overlapping square area. The clipped laps were placed on aluminium foil and heated using a heat gun for 30 s. The laps were allowed to cool for 5 min before the clips were carefully removed and the adhesion of the stuck laps were tested using a Mark-10 tensile tester at a constant up speed of 1.1 mm min^{-1} .

Nuclear magnetic resonance (NMR) spectroscopy

^1H NMR was performed on ternary eutectic mixtures in the absence of crosslinker to monitor the concentrations of NIPAm and Am within polymers formed from these mixtures. The starting reaction mixture contained 3:1 NIPAm:Am, and with 10 wt% MilliQ water, overall. To this solution was added 0.01 wt% TPO, and either no RAFT agent, or 1.0 wt% BisPAT (overall). These two samples were mixed via vortexing and sonication until the mixtures were fully homogeneous. The concentration of TPO was reduced in this experiment to provide practical times for polymerization, sampling, and analysis.

Reactions were performed by pipetting 100 μ L of the ternary eutectic resins into a 2 mL size exclusion chromatography vial, then placing the sealed vial onto a glass slide that was positioned on top of an inverted ThorLabs 405 nm LED with collimation adaptor. The light intensity of the LED was measured to be 0.81 mW cm^{-2} at the bottom surface of the vial. The LED light was then switched on for a designated time to let the photopolymerization proceed. At the end of the allotted time, the LED was switched off and the vial was filled immediately with 800 μ L of deuterated DMSO to stop the reaction, and then re-sealed. The DMSO-polymer solution was then shaken and heated at $50 \text{ }^\circ\text{C}$ for 4 h to aid in dissolution, followed by immersion in a sonic bath for 10 min to further aid in dissolution. Subsequently, the DMSO-polymer solutions were transferred to NMR tubes and analyzed by a Bruker AVANCE III 400 spectrometer (400 MHz, 5 mm BBFO probe). For the no RAFT sample, after 300 s of irradiation the resulting polymer could no longer be solubilized in the solvent and no further time points were taken. The sample containing 1.0 wt% BisPAT was run for twice this time (600 s), however, the polymer was still soluble at this time.

Determination of the individual and total conversion for all samples was performed using the following approach: All samples were phase adjusted and baseline corrected prior to analysis. The integral of the acrylamide vinyl bond methylene proton ($1H$) in the range of 5.565 – 5.620 ppm was measured and set to a value of 1.000. The integrals of three other peaks was then taken: the peak in the range from 1.800-2.400 ppm representing the polymer backbone methine protons ($1H$); the peak in the range of 3.680-4.150 ppm representing the monomer and polymer NIPAm amide NH ($1H$); and the peak in the range of 6.500-7.700

ppm representing the Am monomer and polymer amide NH_2 ($2H$). The NIPAm conversion was taken by first calculating the relative polymer concentration in the mixture, taken as the integral in the range of 3.680-4.150 ppm minus the integral of the peak in the same range from the time = 0 sample (i.e., [polymer]/[monomer + polymer]). The conversion was then determined by this value divided by the total value of the same integral at time = t. The conversion of Am was taken in the same way, by using the ratios of the integrals of the peaks 6.500-7.700 ppm at time = 0 and time = t. The total conversion of the mixture was calculated by taking the weighted sums (by mol) of the monomer conversions from NIPAm and Am and dividing by the total sum of the monomer+polymer $1H$ protons on Am and NIPAm. The conversions of the individual monomer concentrations were plotted against the total conversion, as shown in **Figure S8**. After the reaction at the highest time point for both the no RAFT samples, the mixture became too gelled to analyse properly using these conditions, hence, this analysis is limited to the starting ~25% conversion overall.

The estimation of the reactivity ratios was performed by applying the equations of Lynd and coworkers.¹ These equations (**Eq. S1 and S2**) were solved in Microsoft Excel using the GRG nonlinear engine, with the constraints being minimization of the sum of squares of the difference between the estimated exponent and the value calculated from the NMR analysis. This analysis was performed to provide a rough estimation of the reactivity ratios for comparative purposes.

$$\frac{A_t}{A_0} = \left(\frac{B_t}{B_0}\right)^{r_2} \quad \text{Eq. S1}$$

$$\left(\frac{A_t}{A_0}\right)^{r_1} = \frac{B_t}{B_0} \quad \text{Eq. S2}$$

The values from the NMR analysis for both the no RAFT and 1.0 wt% BisPAT systems, along with an example 1H NMR spectrum used in calculation are shown in **Figure S9**. In **Eq. S1 and S2**, A and B refer to Am and NIPAm, respectively. From this analysis, r_1 and r_2 values were estimated; r_1 refers to the ratio for NIPAm ($k_{NIPAm-NIPAm}/k_{NIPAm-Am}$) and r_2 for Am ($k_{Am-Am}/k_{Am-NIPAm}$). For the no RAFT system the values were: $r_1 = 0.55$ and $r_2 = 1.83$. For the 1.0 wt% BisPAT system the values were: $r_1 = 0.51$ and $r_2 = 1.97$. These values indicate that the Am units have a greater tendency to polymerize with itself than with NIPAm, while NIPAm has a greater tendency to polymerize with Am rather than itself. The findings are in alignment with the preferential incorporation of Am into polymer chains in the early stages of polymerization and the formation of different macromolecular network topologies.

Dynamic mechanical analysis (DMA)

Dynamic mechanical analysis (DMA) of 3D printed specimens was performed using single cantilever mode on a TA Q800 dynamic mechanical analyser. Specimens were 3D printed with designed dimensions of $L \times W \times T = 40 \times 8 \times 2$ mm. The actual dimensions were measured with a digital calliper. The experimental method was applied for all specimens as follows: temperature ramp to 195 °C at 2 °C min⁻¹, constant frequency of 1 Hz and displacement of 15 µm. The glass transition temperature (T_g) was determined using the temperature at the peak of the tan δ curve. DMA measurements were performed in duplicate, with error (\pm) calculated as the standard deviation, calculated in Microsoft Excel using the stdev.p function.

Tensile testing

Dog-bone specimens were designed by modifying the ASTM D638 Type I specimen. Specimen dimensions were: thickness (T) = 2.0 mm, width overall (WO) = 9.6 mm, length overall (LO) = 40 mm, distance between grips (D) = 27.5 mm, gauge length (G) = 10.8 mm, width at the center (W_c) = 3.2 mm. A Mark-10 tensile tester featuring a 1 kN force gauge was used to determine the stress-strain behavior, operating at a constant up-speed of 1.1 mm min⁻¹. Tensile testing measurements were performed in triplicate, with error (\pm) calculated as the standard deviation, calculated in Microsoft Excel using the stdev.p function.

Swelling experiments

Room temperature (22 °C) swelling experiments were performed on 3D printed PE disks with designed diameters of 8 mm and thickness of 1 mm. The disks were measured individually ($d \times t$) using digital callipers, then individually weighed and placed in separate 20 mL vials containing 15 mL of deionized water to meet infinite dilution conditions.² For each set, i.e., no-RAFT vs 0.5 wt% BisPAT vs 1.0 wt% BisPAT, each of the 5 samples was measured at the same swelling time. Samples were carefully removed from the vials using a spatula and tweezers, patted dry with lintless tissues to remove the surface water, immediately weighed, then returned to the same vial. The sample mass appeared to plateau after 24 h and so the disks were remeasured ($d \times t$) using digital callipers. N.B. there is a greater amount of error in the sample size after 24 h swelling, particularly the thickness, due to the increased softness of the disks. For swelling experiments performed at 50 °C, the same general procedure was followed, however, the vials containing DI water and the 3D printed PE disks were placed in an incubator set to 50 °C and only removed during sampling.

Fitting was performed using the equations from Peppas and coworkers.²⁻⁴ The Korsmeyer-Peppas mass transfer model (Eq. S3) was used to determine the mechanism of PE swelling:

$$\frac{M_t}{M_\infty} = K \cdot t^n \quad \text{Eq. S3}$$

Where M_t and M_∞ are the mass at time t and at equilibrium, respectively, K is a complex term representing the diffusion constant, and n is an exponent which details the mass transport behaviour. Data was plotted and fitted in GraphPad Prism and the shaded error bars shown in Figure 5 represent 99% confidence intervals.

Swelling under acidic conditions

Samples for the swelling in low pH media were placed in a solution of HCl in deionized water, made to a final solution pH of 1.0. In individual vials, the samples were placed in the vial then the vial was filled with 15 mL of the pH 1.0 solution. Samples were left for 24 h prior to measurement (assumed to be at equilibrium). Samples were swelled at room temperature (22°C). The samples were patted down using a lintless tissue to remove surface water, then the samples were weighed. Each sample (no-RAFT, BisPAT 0.5, and BisPAT 1.0) were measured in triplicate. Values are presented as an average and standard deviation, calculated using the STDEV.P function in Microsoft Excel.

Swelling experiments for sawtooth plot

The same general procedure outlined in the “Swelling experiments” section was followed for the materials analysed via the sawtooth plot. Samples were weighed and placed in vials containing deionized water and periodically removed for weighing. The time that each sample was allowed to equilibrate was 16 h for each 22 °C point (overnight), and 8 h for the 50 °C swelling points. As such, the materials measured at each of these time points may not have fully reached equilibrium during their measurements. For the 50 °C swelling points, the samples were placed back into the 22 °C water and then placed in the incubator, and thus required a slightly increased time to equilibrate at 50 °C. Data shown in Figure 6 are plotted as an average of 3 points, with the error bars showing the standard deviation calculated using the stdev.p function in Microsoft Excel.

Additional Data

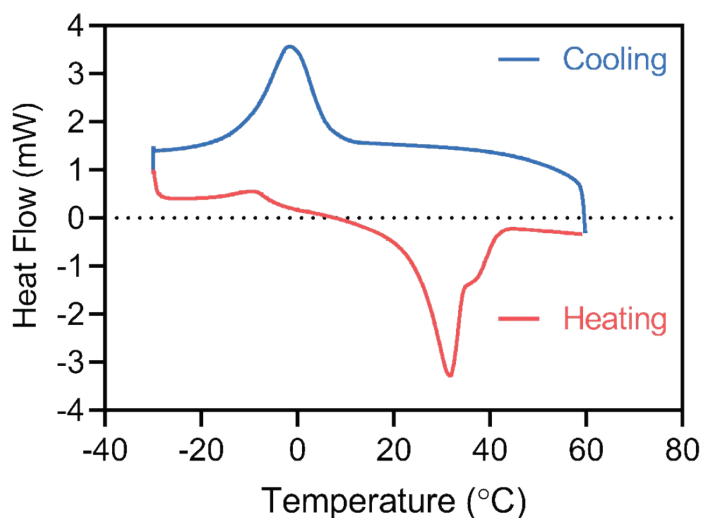


Figure S1. DSC curve for the base mixture (ternary NIPAm/Am/H₂O mixture + 4 wt% overall MBAm). Freezing point was determined to be 6 °C and the melting point was determined to be 24 °C.

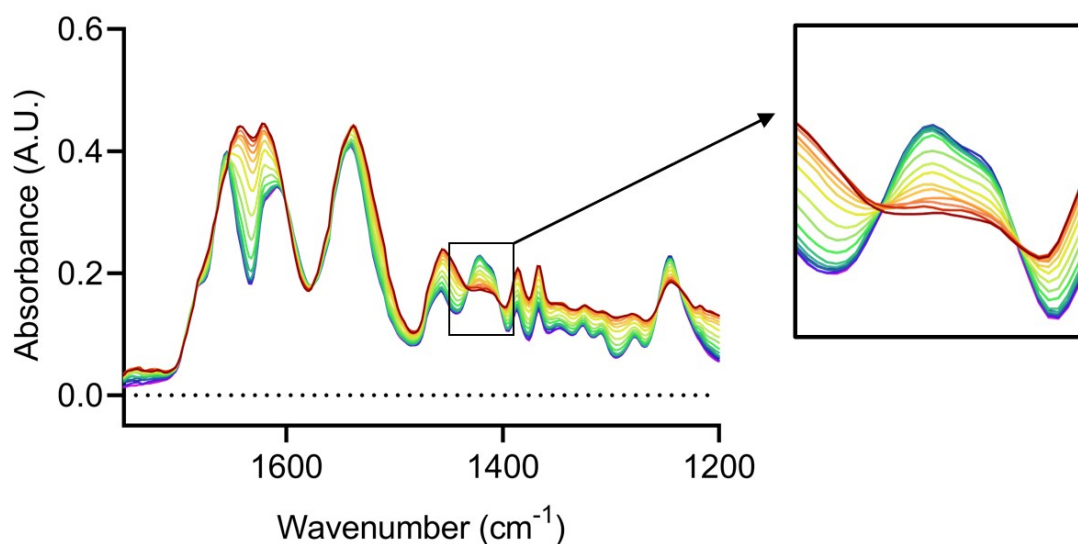


Figure S2. Representative FTIR kinetic set. Blue curve represents start time (0 s) and dark red curves indicate the reaction end time (180 s in this case) Sample is BisPAT 1.0. The inset shows the area of interest used to calculate the conversion. The wavenumber range from 1403-1433 cm⁻¹ was chosen; these values correspond to the isosbestic points either side of the =CH₂ scissoring mode on the vinyl monomers.

Table S1. Droplet polymerization of PE resins using 3D printer light source^a

#	RAFT agent (1 wt%)	TPO concentration (wt%)	Time to cure (s)	Average cure depth ^b (μm)
1	No RAFT	1	15	180
2	No RAFT	2	12	190
3	BisPAT	1	90	90
4	BisPAT	2	60	120
5	CTCPA	1	-	-
6	CTCPA	2	180	90

^a Conditions: 15 μL droplets were pipetted onto glass slides and cured using a 405 nm, 0.81 mW cm^{-2} light source under fully open to air conditions. ^b Average cure depth was calculated by taking the average thickness of three droplets, measured using digital callipers; droplets have variable spreading behaviour based on their viscosity, therefore, these average cure depth values are intended as a guide only.

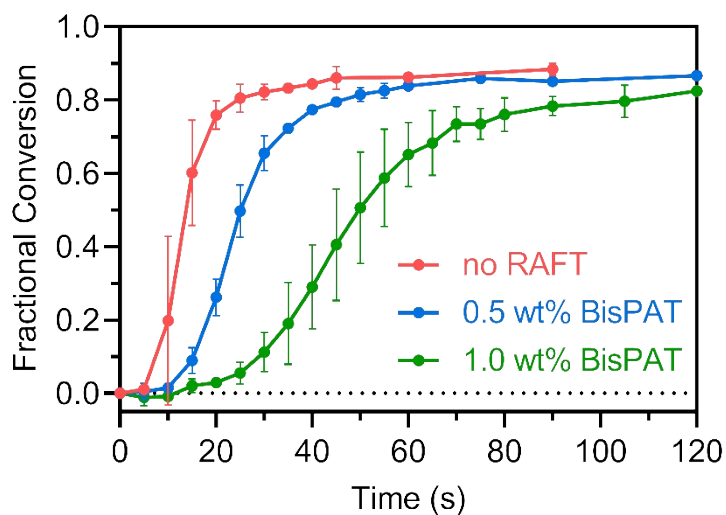


Figure S3. Kinetic plots for the droplet polymerization of no RAFT, 0.5 wt% and 1.0 wt% BisPAT resins. Conversion determined via ATR-FTIR under 0.81 mW cm^{-2} 405 nm light irradiation. Lines are guides for the eye.

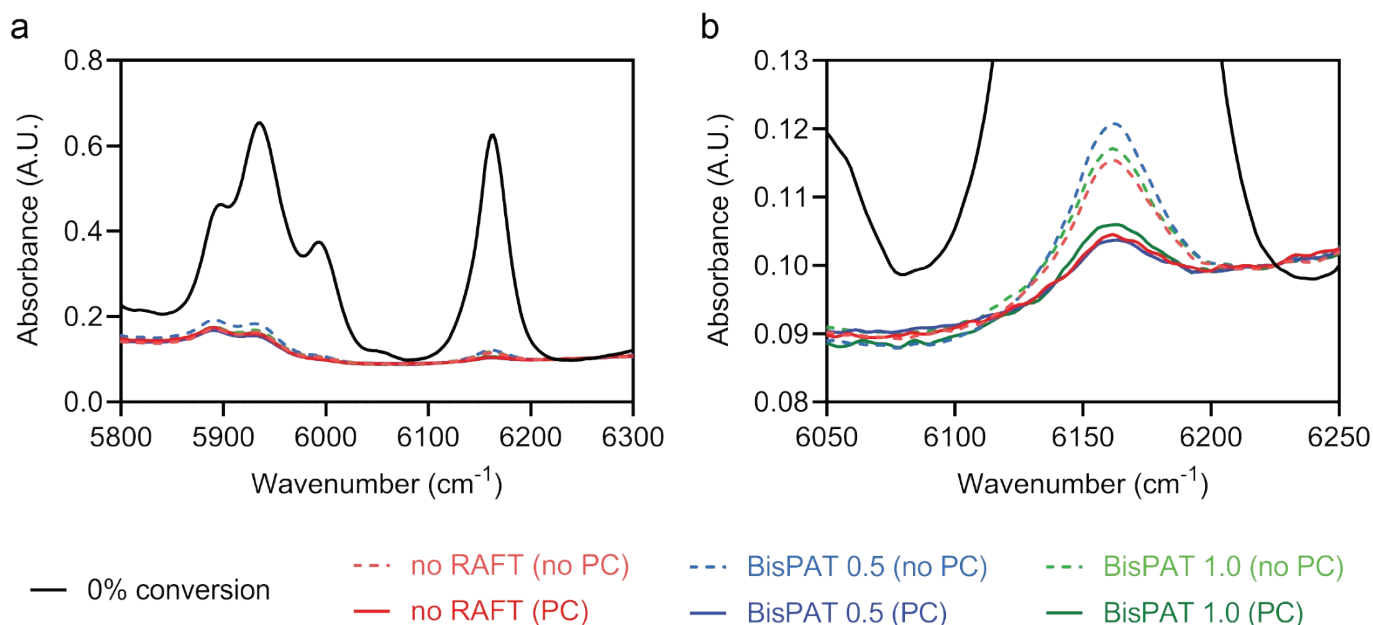


Figure S4. FTNIR for samples before and after post-curing. a) Larger view showing sample before printing (no RAFT resin with 0% conversion, black curve); b) close up view of vinyl C-H stretching overtone at $\sim 6150\text{ cm}^{-1}$ for samples before and after post-curing. Post curing performed by irradiating the samples for 15 min under $\lambda_{\text{max}} = 405\text{ nm}$, $I_0 = 9.6\text{ mW cm}^{-2}$. PC = post-cured, no PC = not post cured (directly after printing and briefly washing with ethanol).

Table S2. Vinyl bond conversion after printing and post curing.^a

Sample#	Conversion after printing (%)	Conversion after post-cure (%)
No-RAFT	96.1	98.2
BisPAT 0.5	94.9	98.5
BisPAT 1.0	95.8	97.7

^a Conversion measured using FTNIR. Samples “after printing” were washed briefly with ethanol, removed from the build stage, and then directly measured. Samples “after post-cure” were washed briefly after printing with ethanol, then post-cured for 15 min under violet light ($\lambda_{\text{max}} = 405\text{ nm}$, $I_0 = 9.6\text{ mW cm}^{-2}$).

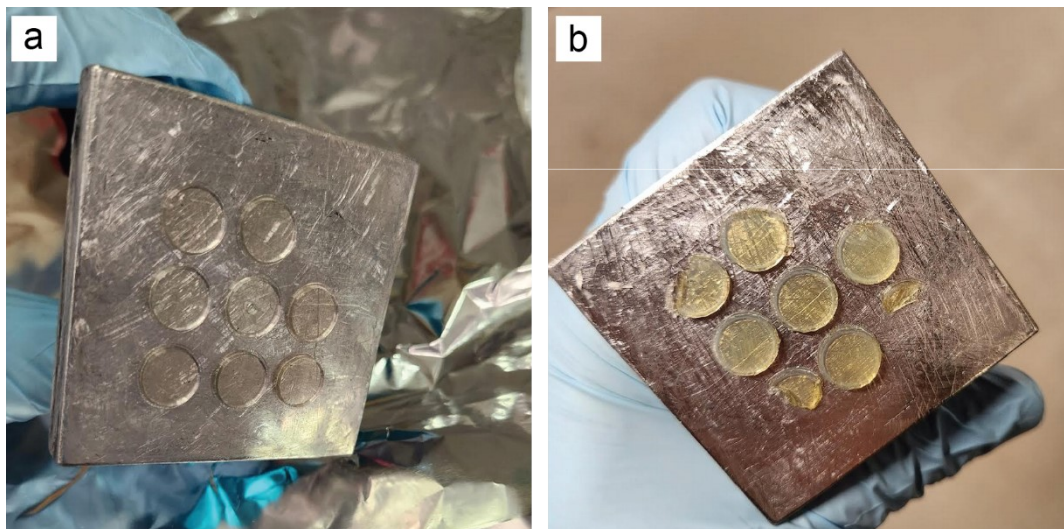


Figure S5. PE disks prepared by 3D printing directly onto the build plate. a) no-RAFT PE resin; and b) 1.0 wt% BisPAT resin showing broken objects after attempts to remove them from the build stage.

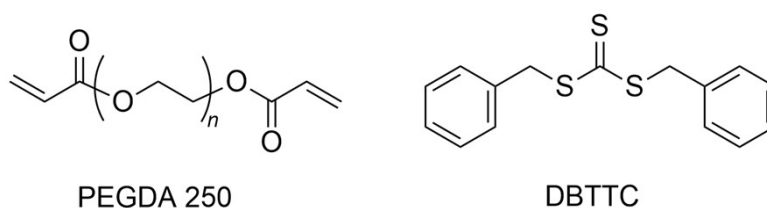


Figure S6. Chemical structures used in control tests for adhesion testing. PEGDA 250: Poly(ethylene glycol) diacrylate, average $M_n = 250$; DBTTC: dibenzyltrithiocarbonate. TPO was also included in at 2 wt% overall.

Table S3. Mechanical properties from DMA for 3D printed PE materials.^a

#	Additive	G' _{glassy} (GPa) ^b	T_g^c (°C) ^c
1	No RAFT ^c	3.2 ± 0.2	130, 152
2	0.5 wt% BisPAT	3.6 ± 0.1	154
3	1.0 wt% BisPAT	4.1 ± 0.8	158

^a Conditions: DMA was performed using a temperature sweep from ambient temperature to 195 °C using a temperature ramp rate of 2 °C min⁻¹, a frequency of 1 Hz and an amplitude of 15 μm; ^b modulus in the glassy state was chosen at the temperature closest to 35 °C; ^c glass transition temperature taken at the temperature where the tan δ curve peaked. The no-RAFT sample showed two distinct T_g at 130 °C and 152 °C.

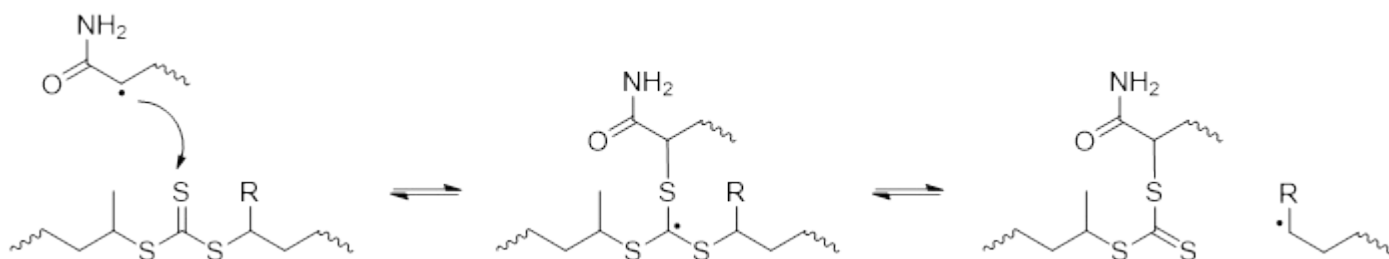


Figure S7. Mechanism of chain transfer and stress relaxation via addition-fragmentation chain transfer using Z-connected RAFT agents such as BisPAT. In the first step, a polymeric radical (with Am or NIPAm terminal unit, drawn as Am here) adds across a thiocarbonyl double bond in the main chain RAFT agent. Fragmentation of the addition product releases another carbon centred radical (adjacent to the R group in this figure). This released radical can migrate via diffusion of the chain end or via polymerization until reaction with another thiocarbonylthio group in another chain. Importantly, the fragmentation step provides an opportunity to relieve stress within the network by allowing stretched chains to adopt a more favourable (less stretched) confirmation. Due to this mechanism, a single radical species is capable of relieving stress in multiple chains via migration of the radical and multiple reactions with thiocarbonyl groups over the lifetime of the radical.

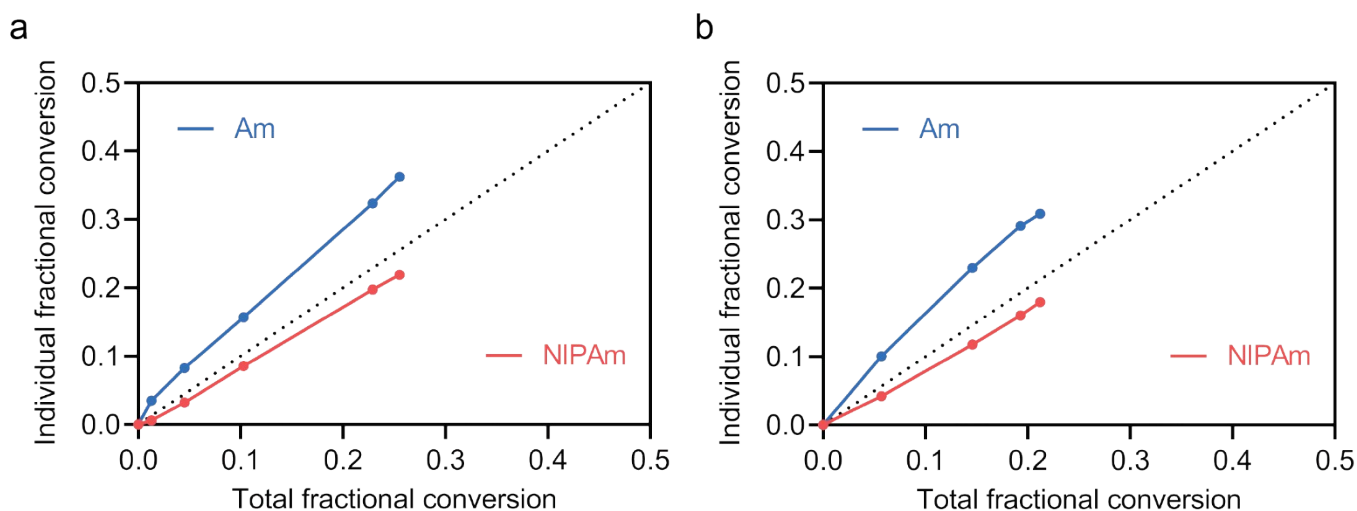


Figure S8. Conversion of NIPAm and Am during their copolymerization. a) Using no-RAFT system with 0.1 wt% TPO; b) using 1.0 wt% BisPAT system with 0.1 wt% TPO. Both systems contained a ternary eutectic mixture comprised of 3:1 NIPAm:Am with an additional 10 wt% water overall. Lines are guides for eye only.

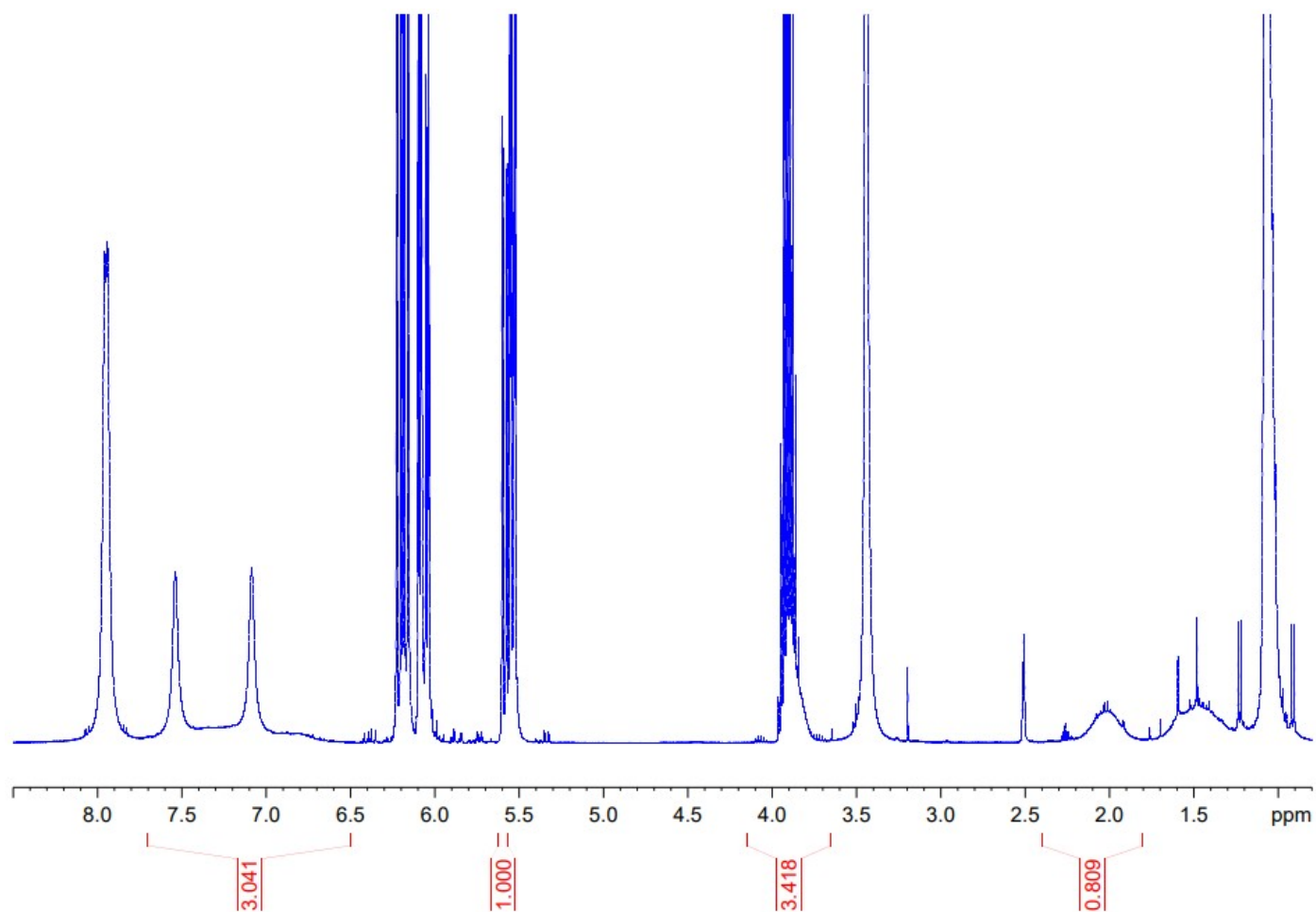


Figure S9. Example of ^1H NMR spectrum and integrals used in the calculation of conversions of individual monomers (NIPAm and Am). This figure represents the 1.0 wt% BisPAT sample irradiated for 600 s under 0.81 mW cm^{-2} 405 nm light. ^1H NMR performed using deuterated DMSO as solvent.

Table S4. Integrals of key peaks from ^1H NMR analysis of conversions of NIPAm and Am during photopolymerization under 405 nm light.^a

Sample	Time (s)	Integral of polymer backbone (1H)	Integral of NIPAm monomer and polymer (1H)	Integral of Am monomer and polymer (2H)	NIPAm conversion	Am conversion	Total conversion
No RAFT	0	0.049	2.817	2.093	0.000	0.000	0.000
	60	0.111	2.835	2.169	0.006	0.035	0.013
	90	0.198	2.911	2.281	0.032	0.083	0.045
	120	0.313	3.081	2.483	0.085	0.157	0.103
	180	0.890	3.510	3.093	0.197	0.323	0.229
	240	1.000	3.606	3.283	0.219	0.363	0.255
BisPAT 1.0	0	0.042	2.803	2.101	0.000	0.000	0.000
	120 ^b	-	-	-	-	-	-
	240	0.209	2.927	2.336	0.042	0.101	0.057
	360	0.539	3.178	2.728	0.118	0.230	0.146
	480	0.758	3.338	2.964	0.160	0.291	0.193
	600	0.809	3.418	3.041	0.180	0.309	0.212

^a Photopolymerization details and calculation of the conversions supplied in the supporting information methods. ^b The conversion of monomer at the 120 s time point for the BisPAT sample was 0% and this result was excluded from the analysis.

Table S5. Am and NIPAm mol% within polymer chains at various total conversions.^a

Sample	Time (s)	Total conversion (%)	Am mol% in polymer	NIPAm mol% in polymer
No RAFT	0	0	-	-
	60	1.3	66.0	34.0
	90	4.5	46.2	53.8
	120	10.3	38.1	61.9
	180	22.9	35.3	64.7
	240	25.5	35.6	64.4
BisPAT 1.0	0	0	-	-
	120 ^b	-	-	-
	240	5.7	44.5	55.5
	360	14.6	39.4	60.6
	480	19.3	37.7	62.3
	600	21.2	36.4	63.6

^a The analysis was performed based on the cumulative mol% of Am and NIPAm within the total chain population. ^b The conversion of monomer at the 120 s time point for the BisPAT sample was 0% and this result was excluded from the analysis.

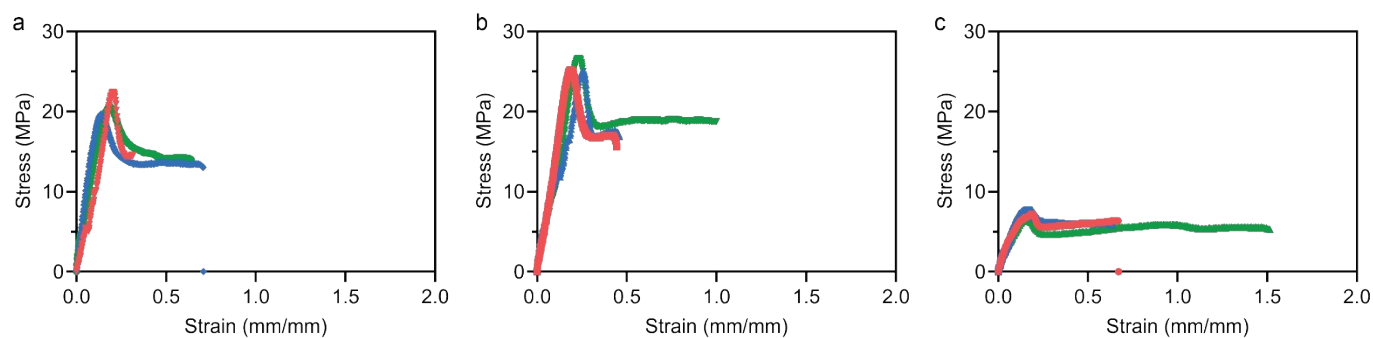


Figure S10. Stress-strain curves for 3D printed PE-RAFT materials. Materials prepared using a) no-RAFT PE resin; b) 0.5 wt% BisPAT PE resin; c) 1.0 wt% BisPAT PE resin. Figures show results from triplicate samples.

Table S6. Mechanical properties from tensile testing of 3D printed PE materials.

#	Additive	E'			Yield stress			Strain at break (mm mm ⁻¹)			Tensile toughness (MJ m ⁻³) ^b		
		(MPa) ^a			(MPa)								
1	No RAFT	160.7	±	52.1	20.9	±	1.1	0.6	±	0.2	7.7	±	2.6
2	0.5 wt% BisPAT	143.2	±	16.2	24.2	±	2.6	0.7	±	0.2	11.4	±	4.6
3	1.0 wt% BisPAT	79.7	±	9.4	7.2	±	0.5	0.9	±	0.4	5.2	±	2.0

^a Young's modulus (E') was calculated as the slope of the stress-strain curve from strain 0.01 mm mm⁻¹ to 0.02 mm mm⁻¹. ^b Tensile toughness calculated as the area under the stress-strain curve. Data represent average of three data points from the data shown in Figure S3. Error values were calculated in Microsoft Excel using the stdev.p function.

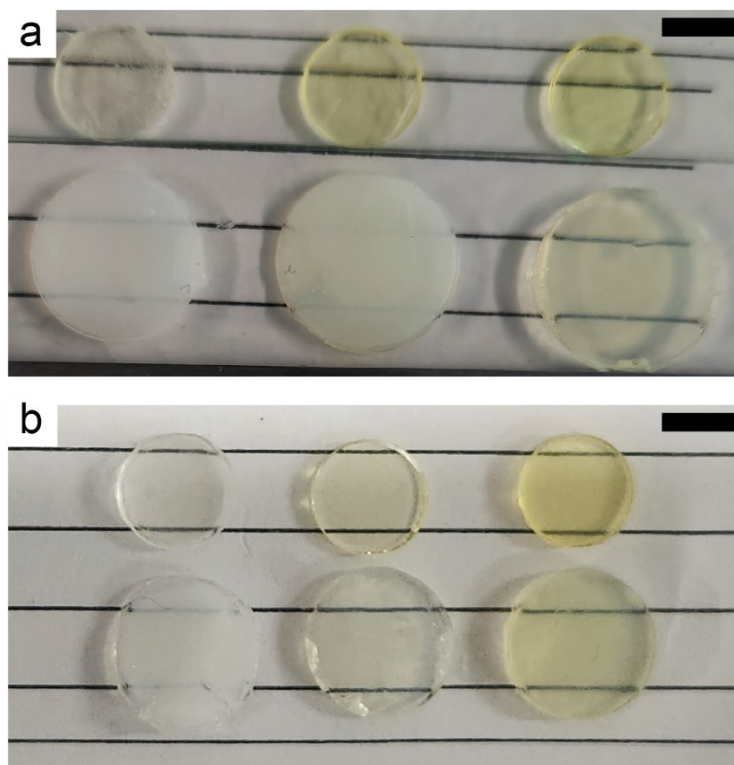


Figure S11. 3D printed PE disks before and after swelling. a) materials before (top) and after (bottom) swelling at 22 °C, from left to right: no-RAFT, 0.5 wt% BisPAT, 1.0 wt% BisPAT; b) materials before (top) and after (bottom) swelling at 50 °C, from left to right: no-RAFT, 0.5 wt% BisPAT, 1.0 wt% BisPAT. Scale bars are approx. 5 mm. Note: Photos in a are not representative of the opacity of every sample and are included to give an indication of general size changes; some no-RAFT and some 0.5 wt% BisPAT samples also had slightly higher transparency, and greater variability in their transparency compared to the 1.0 wt% sample. The photos in b are more representative of the transparency of the actual samples, with the 1.0 wt% samples consistently displaying higher transparency compared to the no-RAFT sample. The 0.5 wt% samples again showed intermediate behaviour, as demonstrated for less transparent samples shown in the swelling of the complex lattice structure.

Table S7. Swelling 3D printed PE materials under acidic conditions.^a

Sample#	Water uptake (g/g)	Standard deviation (g/g)
No-RAFT	2.05	0.02
BisPAT 0.5	2.32	0.04
BisPAT 1.0	2.56	0.02

^a Water uptake for pH 1.0 solutions, swelled for 24 h at room temperature (22°C)

Table S8. Parameters from Peppas model fitting of PE swelling in water.

#	Additive	Temperature (°C)	Parameter from fit	
			K	n
1	No RAFT ^c	22	0.042	0.53
2	0.5 wt% BisPAT	22	0.046	0.49
3	1.0 wt% BisPAT	22	0.043	0.52
4	No RAFT ^c	50	0.047	0.64
5	0.5 wt% BisPAT	50	0.053	0.56
6	1.0 wt% BisPAT	50	0.044	0.54

Supporting Information References

1. B. S. Beckingham, G. E. Sanoja and N. A. Lynd, *Macromolecules*, 2015, **48**, 6922-6930.
2. R. W. Korsmeyer, R. Gurny, E. Doelker, P. Buri and N. A. Peppas, *Int. J. Pharm.*, 1983, **15**, 25-35.
3. R. W. Korsmeyer and N. A. Peppas, *J. Membr. Sci.*, 1981, **9**, 211-227.
4. D. Hariharan and N. A. Peppas, *Polymer*, 1996, **37**, 149-161.